Microbiology (2005), **151**, 323–332 DOI 10.1099/mic.0.27213-0

Changes of the phagosomal elemental concentrations by *Mycobacterium tuberculosis* Mramp

Dirk Wagner,[1] Jörg Maser,[2] Ivana Moric,[2] Neio Boechat,[3] Stefan Vogt,[2] Brigitte Gicquel,[3] Barry Lai,[2] Jean-Marc Reyrat[3]† and Luiz Bermudez[4,5]

[1]Division of Infectious Diseases, Department of Internal Medicine, University of Freiburg, Hugstetter Str 55, 79106 Freiburg, Germany

[2]Experimental Facilities, Argonne National Laboratory, Argonne, IL, USA

[3]Unité de Génétique Mycobactérienne, Institut Pasteur, Paris, France

[4,5]Department of Biomedical Sciences, College of Veterinary Medicine[4] and Department of Microbiology, College of Science[5], Oregon State University, Corvallis, OR, USA

Correspondence
Dirk Wagner
Dirk.Wagner@medizin.ukl.uni-freiburg.de

Pathogenic mycobacteria survive within phagosomes which are thought to represent a nutrient-restricted environment. Divalent cation transporters of the Nramp family in phagosomes and mycobacteria (Mramp) may compete for metals that are crucial for bacterial survival. The elemental concentrations in phagosomes of macrophages infected with wild-type *Mycobacterium tuberculosis* (*M. tuberculosis* strain H37Rv) and a *M. tuberculosis Mramp* knockout mutant (Mramp-KO), derived from a clinical isolate isogenic to the strain MT103, were compared. Time points of 1 and 24 h after infection of mouse peritoneal macrophages (bcg^S) were compared in both cases. Increased concentrations of P, Ni and Zn and reduced Cl concentration in Mramp-KO after 1 h of infection were observed, compared to *M. tuberculosis* vacuoles. After 24 h of infection, significant differences in the P, Cl and Zn concentrations were still present. The Mramp-KO phagosome showed a significant increase of P, Ca, Mn, Fe and Zn concentrations between 1 and 24 h after infection, while the concentrations of K and Ni decreased. In the *M. tuberculosis* vacuole, the Fe concentration showed a similar increase, while the Cl concentration decreased. The fact that the concentration of several divalent cations increased in the Mramp-KO strain suggests that Mramp may have no impact on the import of these divalent cations into the mycobacterium, but may function as a cation efflux pump. The concordant increase of Fe concentrations within *M. tuberculosis*, as well as within the Mramp-KO vacuoles, implies that Mramp, in contrast to siderophores, might not be important for the attraction of Fe and its retention in phagosomes of unstimulated macrophages.

Received 5 April 2004
Revised 16 August 2004
Accepted 7 October 2004

INTRODUCTION

Pathogenic mycobacteria such as *Mycobacterium tuberculosis* and *Mycobacterium avium* survive and replicate within the phagosome, which is thought to be a nutrient-restricted environment important to limit the nutritional needs of phagocytozed microbes. The regulation of the concentration of trace elements in the mycobacterial phagosome, especially of Fe, is known to be of crucial importance for the survival of intracellular organisms (De Voss *et al.*, 2000).

The solute carrier family 11 member 1, Slc11a1, natural-resistance-associated macrophage protein 1 (Nramp1), is assumed to regulate the intraphagosomal replication of unrelated pathogens (mycobacteria, *Salmonella* and *Leishmania*) by controlling divalent cation concentrations at that site (Govoni & Gros, 1998). Polymorphisms in and around the *Nramp1* locus have been genetically linked to the susceptibility to acquire and develop tuberculosis (Awomoyi *et al.*, 2002; Bellamy *et al.*, 1998) and leprosy (Abel *et al.*, 1998) in humans. Nramp1, localized to late endosomal/lysosomal membranes, is a divalent cation pump (Barton *et al.*, 1999), but whether Nramp1 functions as an efflux pump or as an influx pump is an ongoing debate (Forbes & Gros, 2001; Gomes & Appelberg, 2002; Kuhn *et al.*, 2001). Nramp1 may also act as a fusogen that promotes vesicle fusion, resulting in recruitment of vacuolar

†Present address: Faculté de Médecine Necker-Enfants Malades, Paris, France.

Abbreviations: Mramp, homologue of Nramp in *Mycobacterium tuberculosis*; Mramp-KO, Mramp knockout mutant; Nramp, natural-resistance-associated macrophage protein.

H^+-ATPase activity (Hackam *et al.*, 1998). Therefore, it is possible that Nramp1 recruitment may increase the fusogenic properties of mycobacterial phagosome (Forbes & Gros, 2001). Finally, Nramp2 has been implicated as a mediator of microtubule-dependant phagosome and/or lysosome transport (Tokuraku *et al.*, 1998). Co-localization of mycobacterial phagosomes with the Nramp1 protein has only been shown in some, but not all *M. avium*-containing phagosomes (Searle *et al.*, 1998), but it clearly affects intracellular survival of *M. avium* in bone marrow-derived mouse macrophages (Frehel *et al.*, 2002).

In mammals, a second homologue, Nramp2 (DCT1/DMT1), is expressed in many different cells in contrast to the macrophage-/monocyte-specific Nramp1. In intestine and other tissues, Nramp2 is involved in Fe transport (Gruenheid *et al.*, 1999); however, studies in *Xenopus laevis* oozytes have demonstrated that Nramp2 might transport a broad range of divalent metals (Gunshin *et al.*, 1997; Picard *et al.*, 2000; Tandy *et al.*, 2000). In macrophages, Nramp2 is primarily detected in recycling endosomes and also, to a lesser extent, at the plasma membrane, co-localizing with transferrin. It suggests a role for transporting Fe^{2+} into the cytoplasm after acidification of the transferrin-positive endosome (Gruenheid *et al.*, 1999). Although co-localization studies for mycobacterial phagosomes and Nramp2 are missing, the differential regulation of both *Nramp1* and *Nramp2* mRNA following infection with *M. avium* (Zhong *et al.*, 2001) suggests a role of these transporters in the host defence and cation homeostasis.

Nramp homologues have been identified in many different species, including bacteria, with a remarkable degree of phylogenetic conservation (Agranoff *et al.*, 1999; Cellier *et al.*, 2001; Reeve *et al.*, 2002). The homologue in *M. tuberculosis* (Mramp) may be involved in Zn and Fe transport, but it may also interact with a far broader range of divalent transition metal cations (Agranoff *et al.*, 1999). The similarity to enterobacterial MntH has led to the assumption that it is mainly an Mn^{2+} transporter (Domenech *et al.*, 2002). Inactivation of mycobacterial *Mramp* does not affect virulence in mice, suggesting a sufficient redundancy in the cation acquisition systems (Boechat *et al.*, 2002; Domenech *et al.*, 2002). The detection of *Mycobacterium bovis* BCG *Mramp* mRNA in infected THP1 phagocytes, however, implies an intracellular function (Agranoff *et al.*, 1999). Moreover, the manner by which Mramp contributes to the homeostasis of the cation and anion concentrations in the mycobacterial phagosome is unknown. In addition, which of the cations is intracellularly transported by Mramp during infection of mammalian cells has not been studied to date.

Recently, we have established a method to directly measure the local concentration of different elements inside infected phagosomes. Twenty atomic species can be measured and quantified simultaneously without physical sectioning of the specimen and without need for additional staining, such as the use of fluorescent dyes (Cai *et al.*, 2000). Using this approach, that combines high elemental sensitivity (sub-femtogram) and low background with high spatial resolution (150 nm), we have shown that *M. tuberculosis* and *M. avium*, but not the avirulent *Mycobacterium smegmatis*, accumulate Fe in the phagosome, at least in part, through the activity of the transferrin receptor. We have also shown that siderophore production is necessary to retain Fe in the mycobacterial phagosome (Maser *et al.*, 2003; Wagner *et al.*, 2005). In the present study, we have used a hard X-ray microprobe to compare the elemental concentrations in phagosomes infected with wild-type *M. tuberculosis* and an *Mramp* knockout mutant (Mramp-KO). Our data showed that, during infection, the concentration of several divalent cations in the phagosome is increased by the absence of the *Mramp* gene, indicating that Mramp may function as a cation exporter. The concentration of Fe, however, appears not to be affected.

METHODS

Mycobacteria and culture conditions. *Mycobacterium tuberculosis* H37Rv was purchased from ATCC and the Mramp mutant of *M. tuberculosis* (a clinical isolate isogenic to strain MT103) was created as described previously (Boechat *et al.*, 2002). The bacteria were cultured as reported previously (Boechat *et al.*, 2002) in Middlebrook 7H9 broth (Difco) or on Middlebrook 7H11 agar (Difco).

Comparison between H37Rv and MT1O3 strains. To determine whether H37Rv and MT1O3 strains replicated similarly in macrophages, mouse peritoneal macrophages from C57BL/6 (bcg^S) mice were isolated as described previously (Bermudez *et al.*, 1997). Macrophages in culture with RPMI 1640 supplemented with 10 % fetal bovine serum (FBS; Sigma) for 2 days were infected with either MT103 or H37Rv at a ratio of 10 bacteria to 1 macrophage. Uptake was allowed to occur for 1 h and then extracellular bacteria were removed by washing twice with Hank's Balanced Salt Solution (HBSS). Macrophage monolayers were lysed up to 7 days after infection to determine the number of intracellular bacteria, as described by Wagner *et al.* (2002). Supernatants of infected and control macrophages were also collected and assayed for both TNF-α and p70 interleukin-12 (IL-12) by using commercial kits (Biosource International) according to the manufacturer's instructions. The assays had a sensitivity of 5 and 4 pg ml^{-1}, respectively.

Specimen preparation. Mouse peritoneal macrophages from C57BL/6 (bcg^S) mice (10^6 cells) were seeded on 200-mesh, Formvar-coated London finder gold grids (Electron Microscopy Sciences) and cultured for 24 h in RPMI 1640 supplemented with 10 % FBS. The monolayers were infected with either *M. tuberculosis* (strain H37Rv) or the Mramp-KO strain of *M. tuberculosis* for 1 h with an approximate ratio of 10 bacteria per macrophage. After 1 h of infection, the macrophages were washed twice with HBSS to remove the remaining extracellular bacteria, then either fixed in 1 % paraformaldehyde (pH 7·2) for 30 min or kept for 24 h in RPMI 1640 supplemented with 10 % FBS before washing and fixation. This yielded time points of 1 and 24 h after infection. The remaining paraformaldehyde was removed by washing twice with HBSS. The grids were subsequently rinsed briefly with sterile water, air-dried and then kept at room temperature in viewing chambers for the microscopic identification of bacteria or phagosomes by phase microscopy using a Nikon microscope with a PlanApo 60 × /1·3 oil immersion lens.

Hard X-ray microprobe and allocation of the phagosome. A hard X-ray microprobe (Cai *et al.*, 2000) was used to collect

quantitative maps of the elemental distribution in the macrophage and the phagosome. Details regarding data collection have been described previously (Maser *et al.*, 2003). Prior to X-ray imaging, the specimen was previewed by an optical microscope and *x*/*y* coordinates for each phagosome were recorded. The specimen was then placed in the hard X-ray microprobe. An incident photon energy of 10 keV was chosen, which allowed measurement of Zn and lighter elements. Each phagosome, based on the previously measured coordinates, was positioned into the focused X-ray spot and raster-scanned. For all Mramp-KO specimens, a full X-ray fluorescence spectrum was acquired at each pixel of the scan. For *M. tuberculosis* specimens, 10 elemental channels were collected as reported previously (Maser *et al.*, 2003; Wagner *et al.*, 2005).

Data analysis. Elemental maps for Mramp-KO specimens were extracted from the X-ray fluorescence spectra using the software package MAPS (Vogt, 2003; Vogt *et al.*, 2003). Quantification was achieved by measuring X-ray fluorescence from NIST thin-film standards NBS1832 and NBS1833 (National Bureau of Standards, Gaithersburg, USA) prior to, during and after each experiment. A calibration curve was extracted from the calibration standards and subsequently applied to quantify all elements from Na to Zn. The calibration curve was based on direct quantification of elements Si, Ca, K, Ti, V, Mn, Co, Cu, Fe and Zn, interpolation for elements P, S, Cl, Cr and Ni, and extrapolation for Na and Mg. For improved accuracy, the mean elemental content for each mycobacterium was calculated in the following process: in each scan, both the area of the mycobacterium and an area representative of the local cellular background were identified. From fitting these mean spectra and comparison to the calibration curve, raw elemental concentrations were calculated for each mycobacterium and a defined background region. The background signal was estimated by determining the content of the cytoplasm in the very proximity (within 400–600 nm) of the phagosome. We used this signal as a representation of the content of the cytoplasm above and below the phagosome. The net elemental content of each bacterium was then calculated by subtraction of the elemental background of the cell from the raw elemental content of the bacterium. The resulting data were obtained as area density and expressed as $\mu g\ cm^{-2}$. These values can be calculated as $mM\ l^{-1}$ or $\mu M\ l^{-1}$ by using the molar mass of the respective elements and the thickness of the mycobacteria, which we assumed to be 1 μm. At fixed excitation energy, the sensitivity of the measurements is reduced for lighter elements due to both smaller X-ray fluorescence yield and smaller absorption cross-section (Jenkins *et al.*, 1995; Thompson *et al.*, 2001). Therefore, only relatively large concentrations of P, S and Cl can be detected. Sensitivity to Na and Mg is even smaller. Sensitivity to trace metals such as Fe, Mn, Cu and Zn, however, is very high.

Previously data collection on *M. tuberculosis* phagosomes (Wagner *et al.*, 2005) did not allow us to save the full spectra at each pixel. This led to a reduction in sensitivity to Ca in the presence of high K concentrations and did not allow quantification of P, S, Cl and Ni as area density. The concentration of these elements is expressed in normalized counts (photon counts per second of data acquisition time and synchrotron current) to allow comparison of the data.

Statistical analysis of observed elemental changes was performed by comparing the concentration of the respective elements at a specific time point in the different groups (wild-type versus Mramp-KO) and within a group (1 h versus 24 h) using Student's *t*-test. A *P*-value of $<0{\cdot}05$ was considered statistically significant.

RESULTS AND DISCUSSION

The concentration of elements in the phagosome of bacteria ingested by macrophages is thought to be tightly regulated as part of the mechanism of the macrophage to impair bacteria. An example is the delivery of Fe via the transferrin receptor to the phagosome, which is thought to be used to damage bacterial DNA via Fenton catalysis of toxic reactive oxygen species (Henle & Linn, 1997; Kuhn *et al.*, 2001; Wagner *et al.*, 2005; Zhong *et al.*, 2001). At the same time, the macrophage vacuole is thought to reduce the amount of nutrients available to the bacterium in an attempt to impair it by starvation. Possible candidates for the transport of divalent cations from the endosomal system into the cell cytosol are members of the divalent cation transport family of proteins, Nramp1 and Nramp2, that are recruited to phagosomes at different stages of the endosomal continuum (Gruenheid *et al.*, 1999; Searle *et al.*, 1998). Intracellular bacteria, like pathogenic mycobacteria, however, have developed strategies to counteract these lines of attack, such as producing superoxide dismutases or catalases to detoxify reactive oxygen species (Bunting *et al.*, 1998; Escuyer *et al.*, 1996; Piddington *et al.*, 2001), or producing siderophores to acquire Fe (De Voss *et al.*, 2000). Also, the production of metal ion transporters by mycobacteria, like Mramp and heavy metal 'P'-type ATPases, has been implicated in the competition against the deprivation of metal cations (Agranoff *et al.*, 1999; Agranoff & Krishna, 1998). *Mramp* mRNA has been shown to be produced by *M. bovis* BCG after 1 day of infection of THP-1 cells (Agranoff *et al.*, 1999), suggesting a function at that time. Therefore, we conducted a study to directly measure and quantify the concentration of metals in vacuoles of mouse macrophages containing *M. tuberculosis* bacteria in which the *Mramp* gene had been knocked out. The hard X-ray microprobe beamline was calibrated using NIST thin-film standards, which yields a variability of quantification between different experimental runs of less than 10 % (data not shown).

In our study we used macrophages from C57BL/6 (bcg^S) mice. The *Mramp* mutant strain displayed no impairment of growth or survival in $Nramp1^{+/+}$ and $Nramp1^{-/-}$ congenic murine macrophage cell lines (Boechat *et al.*, 2002). Since our study focused on the function of the *Mramp* gene *in vitro*, and since the presence or absence of the *Nramp1* gene does not affect the virulence of the *Mramp* mutant strain, we did not examine the interaction of Mramp with the Nramp proteins in cells expressing a functioning Nramp1 protein.

Evaluation of the ability of H37Rv and MT103 to replicate in mouse macrophages showed that the two bacteria have comparable behaviour (Fig. 1). In addition, the kinetics of induction of TNF-α and IL-12 production were similar for both bacteria (Table 1). Based on these results, we decided to use strain H37Rv as the wild-type control because the availability of hard X-ray microscopy data for this strain is significantly greater.

Experiments were carried out in macrophages infected with the *Mramp* mutant at 1 and 24 h following infection. We used the same time points as in previous experiments

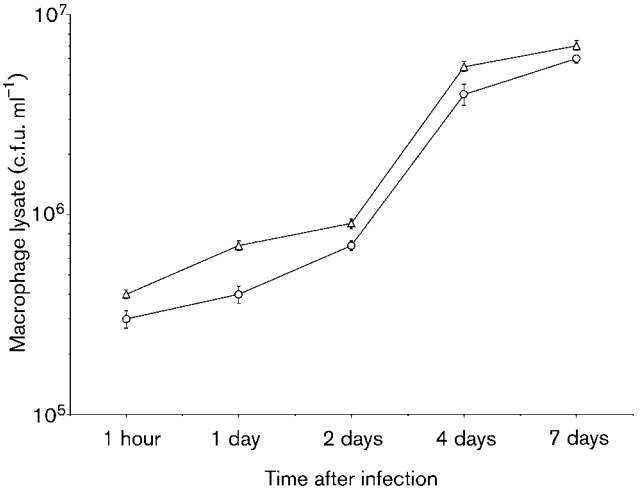

Fig. 1. Comparison between the ability of the *M. tuberculosis* strains H37Rv (circles) and MT103 (triangles) to replicate in C57Bl/6 mouse macrophages.

on *M. tuberculosis*, in which we had observed significant differences in the concentration of several elements in different mycobacterial species (Maser *et al.*, 2003; Wagner *et al.*, 2005). Data for the *M. tuberculosis* wild-type from that study were used (six and seven mapped phagosomes for the 1 and 24 h time points, respectively) as a comparison for the *Mramp* mutant. In this mutant, nine different phagosomes in different macrophages from two different preparations were mapped for each time point. Fig. 2 shows an optical differential interference contrast image of an infected macrophage (Fig. 2a), the elemental distribution of Cl in the macrophage (Fig. 2b) and elemental distributions and X-ray fluorescence spectra of one individual phagosome (Fig. 2c–e). Table 2 lists the different concentrations of the elements in the vacuoles of these mycobacteria and Fig. 3(a–e) shows a schematic representation of these results for the cations of Ca, Zn, Ni, Mn and Fe. Following 1 h of infection, concentrations of P, Ni and Zn were significantly increased in the Mramp-KO strain compared to the wild-type strain, while the Cl concentration decreased. At the 24 h time point, differences in the concentrations of P, Cl and Zn were still observed when compared to the concentrations in the wild-type phagosome after 1 day of infection. At this time point, concentrations of Ca were also significantly higher, while the lower K concentration seen in the Mramp-KO strain was close to being significant ($P=0{\cdot}057$).

Table 1. Production of TNF-α and IL-12 upon macrophage infection with *M. tuberculosis* strains H37Rv and MT103

Data are based on 10^5 macrophages per monolayer. The values (pg ml^{-1}) are the means $\pm$ SD of two experiments.

Strain	24 h		48 h	
	TNF-α	IL-12	TNF-α	IL-12
None	Undetectable	Undetectable	Undetectable	Undetectable
H37Rv	205 ± 24	126 ± 35	161 ± 20	58 ± 9
MT103	236 ± 29	118 ± 22	174 ± 18	64 ± 11

When the comparison was made for the Mramp-KO strain after 1 and 24 h of infection, an increase in Ca, Mn, Fe, Zn and P concentrations was measured, together with a decrease in K and Ni concentrations. The decrease in the Cu concentration over the first day of infection was not significant ($P=0{\cdot}07$). We observed a high variation in the K concentration in both wild-type and mutant phagosomes, similar to variances found in extracellular *M. avium* (unpublished data). It is possible that these variances represent different stages of mycobacterial development, asynchrony in the individual phases of bacterial invasion, or surviving and dead bacteria.

Mramp and the phagosomal Fe concentration

An important finding of our study was a concordant behaviour of the Fe concentration in the wild-type and Mramp-KO strains: in both the Fe concentration increased dramatically over time. The increase of Fe concentration in *M. tuberculosis* and the Mramp-KO vacuoles implies that Mramp, in contrast to siderophores, is not important for attraction and retention of Fe in phagosomes of unstimulated macrophages. This observation is in agreement with previous findings showing that the virulence of the Mramp-KO strain is not affected in mice (Boechat *et al.*, 2002; Domenech *et al.*, 2002). In addition, this finding supports the concept that the Fe concentration in the mycobacterial vacuole is important for intracellular survival (De Voss *et al.*, 2000; Maser *et al.*, 2003; Wagner *et al.*, 2005).

The hard X-ray microprobe is capable of discerning very small amounts of elements, in the order of 10^{-16} g Zn, for example, inside the cell. However, current X-ray optics do not provide the spatial resolution required to discriminate between the vacuole and the bacterium. Since the vacuole membrane of the phagosome is very close to the outermost structure of the bacterium, we assume that most of the elements measured are located inside the bacterium. This would imply that the bacterium can somehow model the contents of the phagosome by importing and exporting elements. In fact, assuming that Mramp would transport specific cations within a phagosome during infection of macrophages into the mycobacterium, the concentration of this cation in the phagosome would be low, and a large portion of the cation would be inside the bacterium; the opposite would occur with the mutant. In contrast, if one assumes that Mramp would not transport a specific cation into the mycobacterium, the concentration of this cation in the phagosome would be high initially, but low after some time due to transport to the extraphagosomal environment. The concentration in the bacterium would

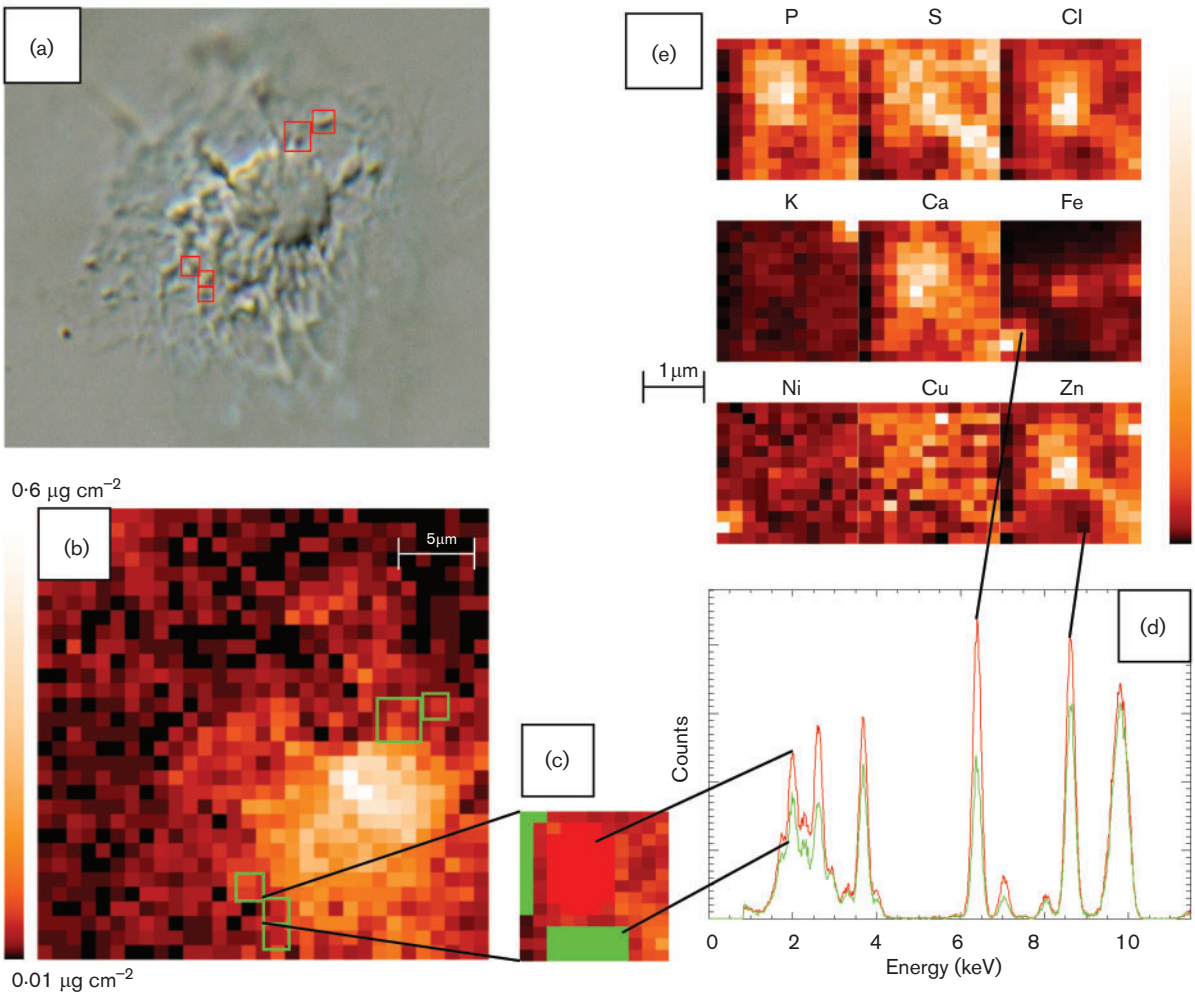

Fig. 2. X-ray map of *M. tuberculosis* Mramp-KO in the hard X-ray microprobe. (a) Optical differential interference contrast image of a macrophage infected for 24 h with *M. tuberculosis*. Areas containing bacterial phagosomes targeted with X-ray scans are highlighted. (b) X-ray map of the macrophage shown in the chloride channel. The same areas with bacterial phagosomes are highlighted. The colour scale represents the range of chloride concentrations from 0·01 (black) to 0·6 μg cm^{-2} (white). Scan area = 31 × 31 μm^2. (c) Area with a single bacterial phagosome. The bacterium is highlighted in red, the background signal of the macrophage outside the phagosome in green. Scan area = 2·2 × 2·2 μm^2. (d) X-ray spectra of bacterial phagosome and the cytoplasmic background. Bacterial spectra are highlighted in red, the cellular background in green. (e) Elemental maps extracted from X-ray spectra. Selected elements are shown. The colour scale corresponds to the range of concentrations of individual elements (μg cm^{-2}): P, 0·56–1·5; S, 0·19–0·53; Cl, 0·15–0·65; K, 0·02–0·19; Ca, 0·06–0·16; Fe, 0·01–1·07; Ni, 0·0001–0·004; Cu, 0·001–0·004; Zn, 0·014–0·03.

be low, as observed in vacuoles with *M. smegmatis*, a bacterium that does not retain Fe within the vacuole (Maser *et al.*, 2003) (Fig. 4).

Mramp – a divalent cation transporter?

Our data do not provide conclusive evidence that the *Mramp* gene functions as a divalent cation transporter in the mycobacterium. The knockout of the *Mramp* gene leads to an increase of the phagosomal concentration of several divalent cations, like Ni and Zn, rather than a decrease after the first hour of infection. After 1 day of infection, the Ca and Mn concentration had increased, while the Zn concentration was further increased. This implies a transport from the cytoplasm to the vacuole and accumulation of these cations in the Mramp-KO strain that does not occur in the wild-type. The decrease in the Ni concentration in the Mramp-KO strain after 24 h suggests that Ni had been transported from the vacuole to the cytoplasm by other transporters. Previous transport studies have shown that the Mramp protein transports divalent cations into *Xenopus laevis* oocytes (Agranoff

Table 2. Intravacuolar concentrations of single elements

Macrophages were infected with *M. tuberculosis* H37Rv (wild-type) and Mramp-KO for 1 or 24 h. Data for the different elements were acquired simultaneously for each phagosome; the number (*n*) of measurements is therefore the same for the different elements as given at the bottom of each column. Mean ± SEM are shown. Elements for which standards are available are expressed and mmol l^{-1} or as μmol l^{-1}, assuming a mean mycobacterial thickness of 1 μm. For previously measured data of *M. tuberculosis*, no standard was available for P, S, Cl and Ni. All data for these elements are therefore expressed as counts per second of data acquisition time and synchrotron current (counts s^{-1} A^{-1}). The Ca concentration for the 1 h time point of *M. tuberculosis* was below the sensitivity of the method for each measured phagosome (see Methods).

Element (unit)	1 h		24 h	
	Wild-type	Mramp-KO	Wild-type	Mramp-KO
P (counts s^{-1} A^{-1})	7·05 ± 1·66	17·7 ± 2·08*†	7·13 ± 1·36	39·5 ± 6·22*
S (counts s^{-1} A^{-1})	36·9 ± 5·53	26·7 ± 2·55	23·7 ± 3·90	58·0 ± 29·7
Cl (counts s^{-1} A^{-1})	404·0 ± 56·1‡	68·7 ± 10·4*	197 ± 62·1	47·4 ± 8·29*
K (mmol l^{-1})	19·5 ± 16·9	46·8 ± 6·09†	51·0 ± 28·6	3·3 ± 0·43§
Ca (mmol l^{-1})	0·00 ± 0·00	0·35 ± 0·17†	0·25 ± 0·17	7·49 ± 0·95*
Mn (μmol l^{-1})	14·7 ± 5·20	16·0 ± 3·80†	16·9 ± 10·9	38·4 ± 8·43
Fe (μmol l^{-1})	135 ± 41·8‡	194 ± 67·4†	2680 ± 974	2913 ± 820
Ni (counts s^{-1} A^{-1})	0·15 ± 0·058	5·4 ± 0·64*†	0·07 ± 0·048‖	0·7 ± 0·27
Cu (μmol l^{-1})	426 ± 393	87 ± 16·4§	25 ± 9·52	49 ± 10·5
Zn (μmol l^{-1})	37·8 ± 25·2	504·5 ± 61·1*†	456·8 ± 271	1057 ± 118*
	n = 7	*n* = 9	*n* = 6	*n* = 9

*$P < 0·05$ versus wild-type (same time point).
†$P < 0·05$ versus Mramp-KO, 24 h.
‡$P < 0·05$ versus wild-type, 24 h.
§$P = 0·057$ versus wild-type, 24 h.
‖$P = 0·07$ versus Mramp-KO, 24 h.

et al., 1999). This does not exclude the possibility that the Mramp protein in the mycobacterial membrane is in an orientation that would lead to an export of these cations, like Ca, Mn, Ni or Zn, out of the mycobacterium. A similar debate is ongoing about the direction of the Nramp1 cation transport in the phagosomal membrane (Forbes & Gros, 2001; Gomes & Appelberg, 2002; Kuhn *et al.*, 2001). In this case, the missing Mramp protein in knockout mutants would lead to an accumulation of these cations, which could have been transported to the phagosome and into the mycobacterium by other cation transporters. In the wild-type, with lower concentrations of Ca, Mn, Ni and Zn, the Mramp protein could have transported these cations out of the mycobacterium and other transport proteins could have exported these from the phagosome to the extraphagosomal environment (Fig. 3).

In *Salmonella*, Mramp functions mainly as an Mn^{2+}-uptake pump (Kehres *et al.*, 2000). It is expressed after invasion of macrophages and induced by hydrogen peroxide (which kills the knockout mutant strain more effectively). However, similar to the mycobacterial Mramp, the *Salmonella* Mramp does not affect invasion or survival of the bacterium in macrophages *in vitro* and only slightly impacts on virulence in a mouse model of infection (Kehres *et al.*, 2000, 2002). In our study, we did not observe a decreased Mn uptake in comparison to the wild-type in mouse peritoneal macrophages. However, the Mn concentration was increased in the vacuole of the Mramp-KO strain after 1 day of infection compared to after 1 h of infection, which was not observed in the wild-type. A similar increase in the Mramp-KO strain compared to the wild-type was also seen for Ca and Zn concentrations, implying an increased delivery of these cations to the phagosome infected with the Mramp-KO strain over time. Again, in the wild-type with lower Ca, Mn and Zn concentrations, Mramp could export these cations during the process of infection, thus preventing this accumulation seen in the Mramp-KO strain (Fig. 3). The implication of these regulatory mechanisms is unclear at the moment. The future identification of specific mutants will provide the tools to further dissect such mechanisms.

Mramp – correlation between Cl and pH?

We found a higher Cl concentration in the wild-type phagosome at both time points compared to the mutant, with the largest concentration after 1 h of infection for the

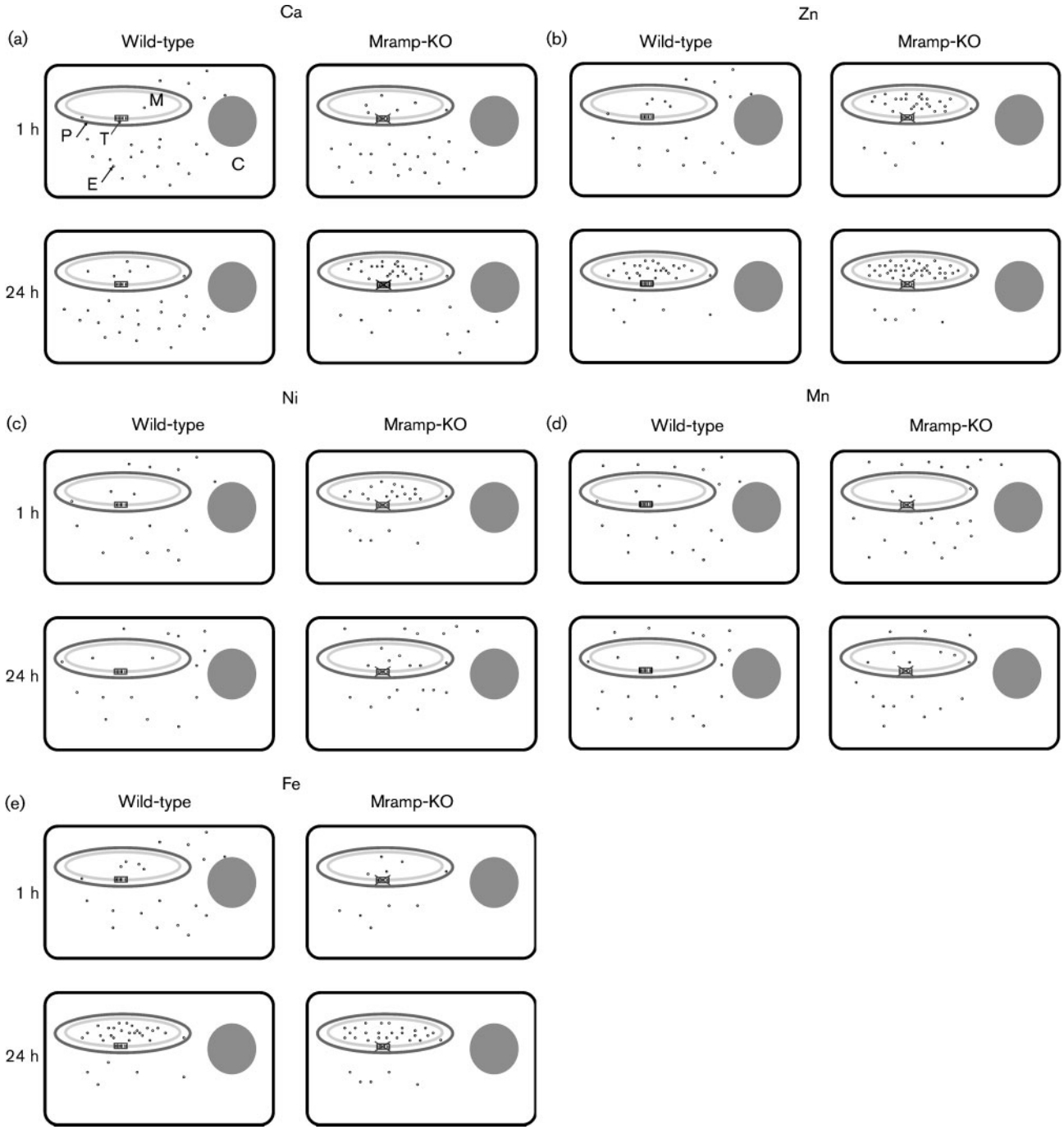

Fig. 3. Schematic representation of the results for the concentration of the cations of Ca (a), Zn (b), Ni (c), Mn (d) and Fe (e). The dots schematically represent the measured concentration of the respective single element (E). Since current X-ray optics do not provide the spatial resolution required to discriminate between the vacuole and the bacterium, the distribution of the concentration of an element between mycobacterium (M) and phagosome (P), and cytoplasm (C) is a presumption (see Fig. 4). T, Mramp transporter. (a) The Ca concentration is low in the wild-type and the Mramp-KO strain after 1 h of infection. It increases significantly after 24 h only in the knockout mutant. (b) The Zn concentration is low in the wild-type and increases significantly after 24 h of infection. In the knockout mutant it is already increased during the first hour and increases further after 24 h. (c) In the Mramp-KO strain, the Ni concentration strongly increased during the first hour and decreased after 24 h, while it stayed low in the wild-type. (d) In the knockout mutant, the Mn concentration stayed low in the wild-type and increased after 24 h in the knockout mutant. (e) The Fe concentration increased dramatically over time in both wild-type and Mramp-KO strains.

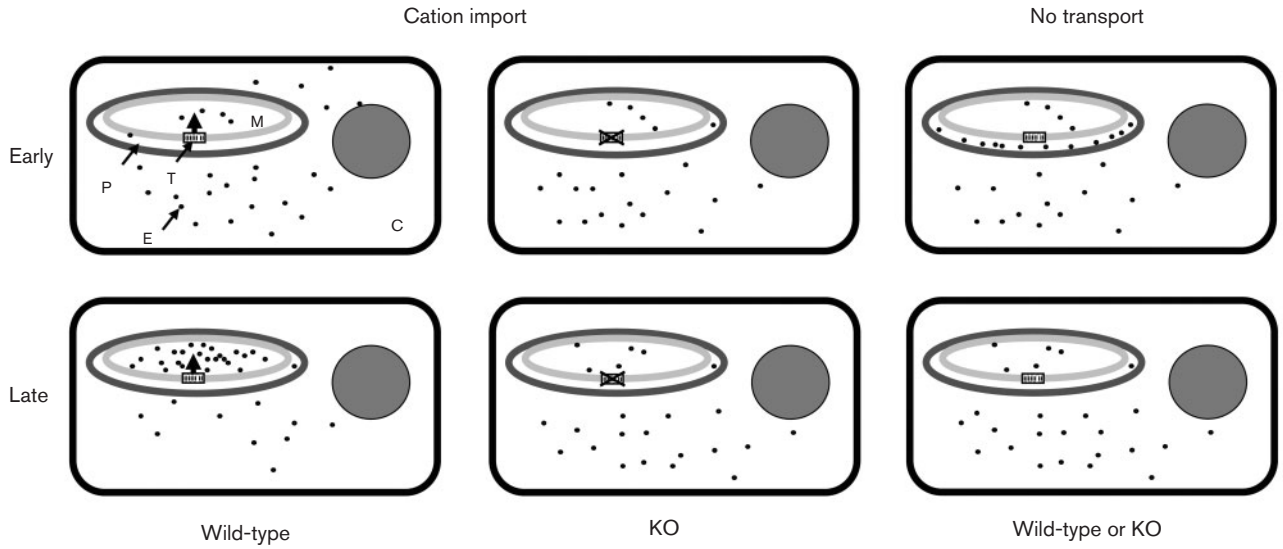

Fig. 4. Schematic representation of the transport of cations by Mramp. Assuming Mramp would function as an importer of specific cations into the mycobacterium during infection of macrophages, the concentration of this cation in the phagosome would be low and a large portion of the cation would be inside the bacterium (left diagrams). In the mutant, where no import takes place, the concentration of this cation in the mycobacterium and the phagosome would be low (middle diagrams). In contrast, if one assumes that Mramp would not transport a specific cation into the mycobacterium, the concentration of this cation in the phagosome could be high initially (provided the cation is transported to the phagosome), but low after some time due to transport to the extraphagosomal environment. The concentration of the cation in the bacterium would be low (right diagrams). M, Mycobacterium; P, phagosome; C, cytoplasm; T, Mramp-transporter; E, elements; arrow, direction of transport.

wild-type and a significantly reduced concentration after 24 h. A recent paper in which the Cl concentration was determined in early and late endosomes using fluorescent ligands suggests that Cl is the principal counter ion accompanying endosomal and Golgi compartment acidification (Sonawane & Verkman, 2003), implying that Cl influx is paralleled by proton influx, and a high Cl concentration may represent a low pH. In mycobacterial phagosomes, a considerable heterogeneity of pH among different vesicles, especially in the first hours of infection, and a detectable initial drop in pH, followed by a recovery and equilibration at pH 6·3–6·5, have been described (Deretic & Fratti, 1999). We speculate that the high initial Cl concentration and the following decrease in the wild-type may reflect this initial drop and later increase of the pH. In the Mramp-KO strain, the accumulation of Cl, especially in the first hours of infection, however, was not observed in this study. The function of Mramp is, similar to other members of this transporter family, supposed to be proton-dependent (Domenech *et al.*, 2002). Provided that Mramp is, as suggested for Nramp1 (Mulero *et al.*, 2002), a divalent cation-proton antiporter and a cation efflux pump (as suggested by our data), it is tempting to speculate that the knockout of this transporter leads to less accumulation of protons in the mycobacterium and concomitantly to a lower Cl concentration. This hypothesis, as well as the question whether the decreased K concentration, seen in the Mramp-KO strain after 24 h of infection, is related to this phenomenon or to the missing efflux of divalent cations, need to be investigated in subsequent, specifically designed experiments.

In conclusion, the concentration of several divalent cations increased in the Mramp-KO vacuole within 1 h and over the 1 day post-infection period, indicating that Mramp may not import divalent cations into the mycobacterium, but rather may function as a cation efflux pump. The concordant increase of Fe concentrations in *M. tuberculosis* and the Mramp-KO vacuoles implies that Mramp, in contrast to siderophores, is not important for the attraction of Fe and its retention in phagosomes of unstimulated macrophages.

ACKNOWLEDGEMENTS

This work was supported by Grant # ROI-AI 47010 of the National Institutes of Health and by the US Department of Energy, Office of Energy Sciences, under Contract No. W-31-109-Eng-38. We would like to thank Dan Legnini for the development of high-precision specimen mounts. We thank Denny Weber for helping to prepare the manuscript.

REFERENCES

Abel, L., Sanchez, F. O., Oberti, J., Thuc, N. V., Hoa, L. V., Lap, V. D., Skamene, E., Lagrange, P. H. & Schurr, E. (1998). Susceptibility to leprosy is linked to the human NRAMP1 gene. *J Infect Dis* **177**, 133–145.

Agranoff, D. D. & Krishna, S. (1998). Metal ion homeostasis and intracellular parasitism. *Mol Microbiol* **28**, 403–412.

Agranoff, D., Monahan, I. M., Mangan, J. A., Butcher, P. D. & Krishna, S. (1999). *Mycobacterium tuberculosis* expresses a novel pH-dependent divalent cation transporter belonging to the Nramp family. *J Exp Med* **190**, 717–724.

Awomoyi, A. A., Marchant, A., Howson, J. M., McAdam, K. P., Blackwell, J. M. & Newport, M. J. (2002). Interleukin-10, polymorphism in SLC11A1 (formerly NRAMP1), and susceptibility to tuberculosis. *J Infect Dis* **186**, 1808–1814.

Barton, C. H., Biggs, T. E., Baker, S. T., Bowen, H. & Atkinson, P. G. (1999). Nramp1: a link between intracellular iron transport and innate resistance to intracellular pathogens. *J Leukoc Biol* **66**, 757–762.

Bellamy, R., Ruwende, C., Corrah, T., McAdam, K. P., Whittle, H. C. & Hill, A. V. (1998). Variations in the NRAMP1 gene and susceptibility to tuberculosis in West Africans. *N Engl J Med* **338**, 640–644.

Bermudez, L. E., Parker, A. & Goodman, J. (1997). Growth within macrophages increases the efficiency of *Mycobacterium avium* to invade other macrophages by complement receptor independent pathway. *Infect Immun* **65**, 1916–1922.

Boechat, N., Lagier-Roger, B., Petit, S., Bordat, Y., Rauzier, J., Hance, A. J., Gicquel, B. & Reyrat, J. M. (2002). Disruption of the gene homologous to mammalian Nramp1 in *Mycobacterium tuberculosis* does not affect virulence in mice. *Infect Immun* **70**, 4124–4131.

Bunting, K., Cooper, J. B., Badasso, M. O., Tickle, I. J., Newton, M., Wood, S. P., Zhang, Y. & Young, D. (1998). Engineering a change in metal-ion specificity of the iron-dependent superoxide dismutase from *Mycobacterium tuberculosis* – X-ray structure analysis of site-directed mutants. *Eur J Biochem* **251**, 795–803.

Cai, Z., Lai, B., Yun, W., Ilinski, P., Legnini, D., Maser, J. & Rodrigues, W. (2000). A hard X-ray scanning microprobe for fluorescence imaging and microdiffraction at the advanced photon source. In *X-ray Microscopy*, pp. 472–477. Edited by T. W. W. Meyer-Ilse & D. Attwood. Melville, NY: American Institute of Physics.

Cellier, M. F., Bergevin, I., Boyer, E. & Richer, E. (2001). Polyphyletic origins of bacterial Nramp transporters. *Trends Genet* **17**, 365–370.

Deretic, V. & Fratti, R. A. (1999). *Mycobacterium tuberculosis* phagosome. *Mol Microbiol* **31**, 1603–1609.

De Voss, J. J., Rutter, K., Schroeder, B. G., Su, H., Zhu, Y. & Barry, C. E. (2000). The salicylate-derived mycobactin siderophores of *Mycobacterium tuberculosis* are essential for growth in macrophages. *Proc Natl Acad Sci U S A* **97**, 1252–1257.

Domenech, P., Pym, A. S., Cellier, M., Barry, C. E., 3rd & Cole, S. T. (2002). Inactivation of the *Mycobacterium tuberculosis* Nramp orthologue (mntH) does not affect virulence in a mouse model of tuberculosis. *FEMS Microbiol Lett* **207**, 81–86.

Escuyer, V., Haddad, N., Frehel, C. & Berche, P. (1996). Molecular characterization of a surface-exposed superoxide dismutase of *Mycobacterium avium*. *Microb Pathog* **20**, 41–55.

Forbes, J. R. & Gros, P. (2001). Divalent-metal transport by NRAMP proteins at the interface of host–pathogen interactions. *Trends Microbiol* **9**, 397–403.

Frehel, C., Canonne-Hergaux, F., Gros, P. & De Chastellier, C. (2002). Effect of Nramp1 on bacterial replication and on maturation of *Mycobacterium avium*-containing phagosomes in bone marrow-derived mouse macrophages. *Cell Microbiol* **4**, 541–556.

Gomes, M. S. & Appelberg, R. (2002). NRAMP1- or cytokine-induced bacteriostasis of *Mycobacterium avium* by mouse macrophages is independent of the respiratory burst. *Microbiology* **148**, 3155–3160.

Govoni, G. & Gros, P. (1998). Macrophage NRAMP1 and its role in resistance to microbial infections. *Inflamm Res* **47**, 277–284.

Gruenheid, S., Canonne-Hergaux, F., Gauthier, S., Hackam, D. J., Grinstein, S. & Gros, P. (1999). The iron transport protein NRAMP2 is an integral membrane glycoprotein that colocalizes with transferrin in recycling endosomes. *J Exp Med* **189**, 831–841.

Gunshin, H., Mackenzie, B., Berger, U. V., Gunshin, Y., Romero, M. F., Boron, W. F., Nussberger, S., Gollan, J. L. & Hediger, M. A. (1997). Cloning and characterization of a mammalian proton-coupled metal-ion transporter. *Nature* **388**, 482–488.

Hackam, D. J., Rotstein, O. D., Zhang, W., Gruenheid, S., Gros, P. & Grinstein, S. (1998). Host resistance to intracellular infection: mutation of natural resistance-associated macrophage protein 1 (Nramp1) impairs phagosomal acidification. *J Exp Med* **188**, 351–364.

Henle, E. S. & Linn, S. (1997). Formation, prevention, and repair of DNA damage by iron/hydrogen peroxide. *J Biol Chem* **272**, 19095–19098.

Jenkins, R., Gould, R. W. & Gedcke, D. (1995). *Quantitative X-ray Spectrometry*, 2nd edn. New York: Marcel Dekker.

Kehres, D. G., Zaharik, M. L., Finlay, B. B. & Maguire, M. E. (2000). The NRAMP proteins of *Salmonella typhimurium* and *Escherichia coli* are selective manganese transporters involved in the response to reactive oxygen. *Mol Microbiol* **36**, 1085–1100.

Kehres, D. G., Janakiraman, A., Slauch, J. M. & Maguire, M. E. (2002). Regulation of *Salmonella enterica* serovar *Typhimurium mntH* transcription by H_2O_2, Fe^{2+}, and Mn^{2+}. *J Bacteriol* **184**, 3151–3158.

Kuhn, D. E., Lafuse, W. P. & Zwilling, B. S. (2001). Iron transport into *Mycobacterium avium*-containing phagosomes from an Nramp1 (Gly169)-transfected RAW264.7 macrophage cell line. *J Leukoc Biol* **69**, 43–49.

Maser, J., Wagner, D., Lai, B., Cai, Z., Legnini, D., Moric, I. & Bermudez, L. (2003). Trace metals and their relation to bacterial infections studied by X-ray microscopy. Proceedings of the Seventh International Conference on X-ray Microscopy. *J Phys IV* **104**, 283–288.

Mulero, V., Searle, S., Blackwell, J. M. & Brock, J. H. (2002). Solute carrier 11a1 (Slc11a1; formerly Nramp1) regulates metabolism and release of iron acquired by phagocytic, but not transferrin-receptor-mediated, iron uptake. *Biochem J* **363**, 89–94.

Picard, V., Govoni, G., Jabado, N. & Gros, P. (2000). Nramp 2 (DCT1/DMT1) expressed at the plasma membrane transports iron and other divalent cations into a calcein-accessible cytoplasmic pool. *J Biol Chem* **275**, 35738–35745.

Piddington, D. L., Fang, F. C., Laessig, T., Cooper, A. M., Orme, I. M. & Buchmeier, N. A. (2001). Cu,Zn superoxide dismutase of *Mycobacterium tuberculosis* contributes to survival in activated macrophages that are generating an oxidative burst. *Infect Immun* **69**, 4980–4987.

Reeve, I., Hummel, D., Nelson, N., Voss, J. & Hummell, D. (2002). Overexpression, purification, and site-directed spin labeling of the Nramp metal transporter from *Mycobacterium leprae*. *Proc Natl Acad Sci U S A* **99**, 8608–8613.

Searle, S., Bright, N. A., Roach, T. I., Atkinson, P. G., Barton, C. H., Meloen, R. H. & Blackwell, J. M. (1998). Localisation of Nramp1 in macrophages: modulation with activation and infection. *J Cell Sci* **111**, 2855–2866.

Sonawane, N. D. & Verkman, A. S. (2003). Determinants of [Cl-] in recycling and late endosomes and Golgi complex measured using fluorescent ligands. *J Cell Biol* **160**, 1129–1138.

Tandy, S., Williams, M., Leggett, A., Lopez-Jimenez, M., Dedes, M., Ramesh, B., Srai, S. K. & Sharp, P. (2000). Nramp2 expression is associated with pH-dependent iron uptake across the apical membrane of human intestinal Caco-2 cells. *J Biol Chem* **275**, 1023–1029.

Thompson, A. C., Attwood, D. T., Gullikson, E. M. & 11 other authors (2001). *X-Ray Data Booklet*, 2nd edn. University of California, Berkeley: Lawrence Berkeley National Laboratory.

Tokuraku, K., Nakagawa, H., Kishi, F. & Kotani, S. (1998). Human natural resistance-associated macrophage protein is a new type of microtubule-associated protein. *FEBS Lett* **428**, 63–67.

Vogt, S. (2003). MAPS: a set of software tools for analysis and visualization of 3D X-ray fluorescence data sets. Proceedings of the Seventh International Conference on X-ray Microscopy. *J Phys IV* **104**, 635–638.

Vogt, S., Maser, J. & Jacobsen, C. (2003). Data analysis for X-ray fluorescence imaging. Proceedings of the Seventh International Conference on X-ray Microscopy. *J Phys IV* **104**, 617–622.

Wagner, D., Sangari, F. J., Kim, S., Petrofsky, M. & Bermudez, L. E. (2002). *Mycobacterium avium* infection of macrophages results in progressive suppression of interleukin-12 production *in vitro* and *in vivo*. *J Leukoc Biol* **71**, 80–88.

Wagner, D., Maser, J., Lai, B., Cai, Z., Barry, C. E., 3rd, Höner zu Bentrup, K., Russell, D. G. & Bermudez, L. E. (2005). Elemental analysis of *Mycobacterium avium, Mycobacterium tuberculosis* and *Mycobacterium smegmatis*-containing phagosomes indicates pathogen-induced microenvironments within the host cell's endosomal system. *J Immunol* (in press).

Zhong, W., Lafuse, W. P. & Zwilling, B. S. (2001). Infection with *Mycobacterium avium* differentially regulates the expression of iron transport protein mRNA in murine peritoneal macrophages. *Infect Immun* **69**, 6618–6624.